Magnetic Phase Diagram of Ce1-xErxAl2 intermetallic compounds

Magnetic Phase Diagram of $Ce_{1-x}Er_xAl_2$ intermetallic compounds

[1]Masashi Ohashi*, [2]Hidenori Miyagawa, [2,3]Gendo Oomi, [4] Tomohito Nakano, [5] Isamu Satoh, [5] Takemi Komatsubara

[1]*Faculty of Engineering, Kanazawa University,Kakuma-machi, Kanazawa 920-1192, Japan*
[2]*Department of Physics, Kyushu University, Ropponmatsu, Fukuoka 810-8560, Japan*
[3]*Kurume Institute of Technology, Kamitsu-machi, Kurume, Fukuoka 830-0052, Japan*
[4]*Faculty of Engineering, Niigata University, Niigata 950-2181, Japan*
[5]*Institute for Materials Research, Tohoku University, Sendai 980-8577, Japan*

(Received October 20, 2013)

The magnetic and thermal properties of $Ce_{1-x}Er_xAl_2$ compounds have been studied using electrical resistivity and magnetic susceptibility measurements. The magnetic ordering temperature continuously changes with a change from antiferro-magnetism ($CeAl_2$) to ferro-magnetism ($ErAl_2$) appears. The magnetic ordering temperature is continuously changed as a function of Er concentration x. A spin glass behavior was found between x= 0.08 and 0.4. The magnetic phase diagram was compiled as a function of x.

KEYWORDS: spin glass, electrical resistivity, susceptibility, $CeAl_2$, $ErAl_2$

1. Introduction

The magnetic properties of intermetallic compounds containing rare-earth elements have been an subject of great interest [1–3]. In particular, the binary compounds of RAl_2 have attracted much attention due to their simple structure. The crystal structure of these compounds is isomorphic with the $MgCu_2$ Laves phase (C15 phase). It belongs to the $Fd\bar{3}m$ group [4]. The rare-earth spins in most RAl_2 compounds are assumed to be parallel to each other so that they become ferromagnetic below Curie temperatures T_C [5, 6]. It is well known that the exchange coupling between the localized $4f$-electron shells of the rare-earth ions is due to the conduction electrons (Ruderman-Kittel-Kasuya-Yoshida interaction). $ErAl_2$ exhibits ferromagnetic ordering at approximately 13 K [7], and the easy axis of $ErAl_2$ is [111].

On the other hand, $CeAl_2$ is a special case among these compounds. Since the f-level of $CeAl_2$ is energetically close to the conduction-electron band, both magnetic and hybridization interactions between f levels and the conduction-electron band are vital for the determination of the ground state. Considerable attention has been focused on $CeAl_2$ as a system that shows the competition between these magnetic and nonmagnetic interactions. An antiferromagnetic ordering due to a spin density wave occurs at T_N = 3.8 K [9–11], while Kondo-type conduction-electron screening of the localized moments occurs above T_N, which is suppressed by applying pressure since T_N is merged to the Kondo temperature T_K [10]. Below T_N, a pronounced jump in the magnetization has been observed at a magnetic field approximately 5 T in a $CeAl_2$ single crystal. It indicates a metamagnetic phase transition from the antiferromagnetic to the paramagnetic ordering phase [12]. At higher magnetic phases, the magnetization curve along the easy axis [111] is the highest.

*E-mail address: ohashi@se.kanazawa-u.ac.jp

In the pseudobinary system $Ce_{1-x}Er_xAl_2$, the substitution of Er by Ce causes changes in the magnetic interaction. Because of the competition between the ferromagnetic interaction of $ErAl_2$ (x = 1) and the antiferromagnetic interaction of $CeAl_2$ (x = 0), we expect to observe interesting magnetic properties by changing the substitution of Er and Ce. In this paper, we present electrical resistivity and magnetic susceptibility for $Ce_{1-x}Er_xAl_2$ with $0 < x < 1$. We also describe the influence of Er substitution on the magnetic properties of the $Ce_{1-x}Er_xAl_2$ system, which presents a complex magnetic phase diagram with anti ferromagnetism, ferromagnetism, and spin-glass states.

2. Experimental method

Single crystals of $Ce_{1-x}Er_xAl_2$ and $LaAl_2$ were grown by Czochralski pulling method from the melt of stoichiometric amounts of the constituent elements in a tetra-arc furnace. All ingots were confirmed as single crystals by means of their Laue pattern. The crystal structures are confirmed to be the cubic C15 Laves phase. The lattice parameter a of $CeAl_2$ and $ErAl_2$ are 8.066 Å and 7.791 Å, respectively, which is comparable with those in the previous reports [4]. For $Ce_{1-x}Er_xAl_2$, a decreases by increasing x, which is due to the lanthanide contraction. The electrical resistivity was measured for current parallel to the [100] axis in the temperature range between 2 and 300 K by a standard four-probe method using copper wires (diameters 50 μm) or gold wires (diameters 20 μm). The dc magnetization was measured at a magnetic field 1 kOe along the easy axis [111] using the Quantum-Design MPMS. The ac magnetic susceptibility was measured at a modulation field of along [111] using the Quantum-Design PPMS.

3. Results

The temperature dependence of the electrical resistivity $\rho(T)$ for $Ce_{1-x}Er_xAl_2$ and $LaAl_2$ is shown in Fig. 1. The $\rho(T)$ changes drastically with the composition x. For x = 0, $\rho(T)$ decreases with decreasing temperature, and shows a peak around 5 K and a shoulder around 60 K due to combination of Kondo effect and crystal field splitting. The ρ at low temperature tends to increase with increasing Er concentration up to x = 0.4. For x = 0.4, the ρ increases down to 2 K with decreasing temperature without the decrease of $\rho(T)$. On the other hand, for x = 0.6 and 0.8, the anomaly of $\rho(T)$ due to the ferromagnetic ordering is observed around T_C= 7.1 K and 9.2 K as the sudden decrease and the kink of $\rho(T)$, respectively. The $\rho(T)$ for x = 1 decreases monotonically with decreasing temperature, and the sudden decrease due to the ferromagnetic ordering is observed below T_C= 13 K.

Fig. 2 (a) shows the magnetic susceptibility χ of $Ce_{1-x}Er_xAl_2$ as a function of temperature. The expanded scale below $x \leq 0.1$ is shown in Fig. 2 (b). For x = 0 and 0.02, the rapid decrease due to antiferromagnetic ordering is observed at 3.9 and 3.3 K, respectively. The $\chi(T)$ for $0.1 < x < 0.4$ increases monotonically with decreasing temperature, and the value of χ is larger than that for $CeAl_2$. It indicates that the ferromagnetic interaction is enhanced by substituting Er. For $x > 0.6$ where the ferromagnetic transition is observed, $\chi(T)$ shows a maximum since all $\chi(T)$ curves in Fig. 2 are taken from the zero field cooling data. T_C corresponds to the inflection point on the $\chi(T)$ curve.

To investigate the magnetic ordering state in depth, we performed the ac susceptibility measurements for several frequencies. Fig. 3 shows a typical example of the temperature dependence on the ac magnetic susceptibility $\chi'(T)$ curve of $Ce_{0.8}Er_{0.2}Al_2$ below 4.0 K for several frequencies. All $\chi'(T)$ of the $Ce_{1-x}Er_xAl_2$ compounds show a similar behavior, which have a single maximum. Here we define T_M which shows a maximum on $\chi'(T)$. As shown in Fig. 3, χ' exhibits pronounced maximum with amplitude and positions depending on the frequency of the applied magnetic field, especially in the low-frequency range. This result indicates the formation of a spin-glass state in $Ce_{0.8}Er_{0.2}Al_2$ with the spin freezing temperature T_M = 2.50 K (at f = 100 Hz).

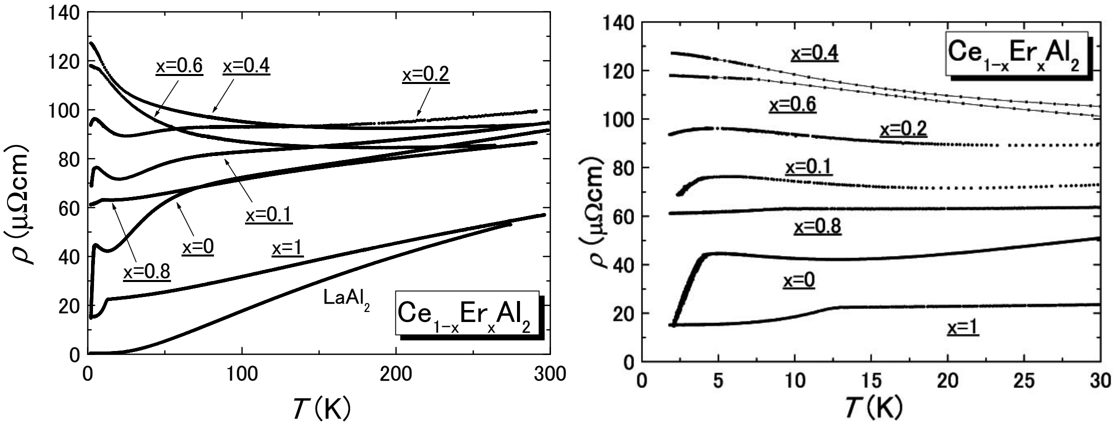

Fig. 1. Temperature depnedence of the electrical resistivity $\rho(T)$ in $Ce_{1-x}Er_xAl_2$. Right plot shows the expanded scale of $\rho(T)$ below 30 K

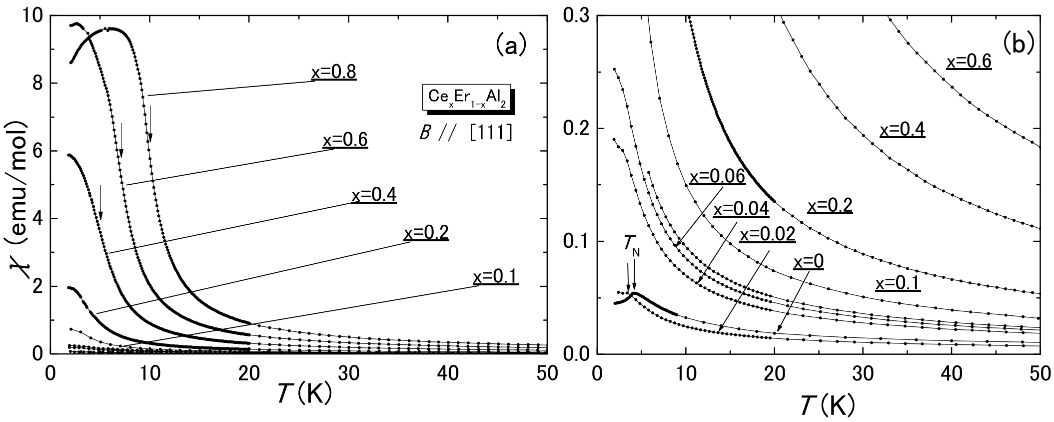

Fig. 2. (a) Temperature dependence of dc susceptibility $\chi(T)$ for $Ce_{1-x}Er_xAl_2$. The arrow shows the inflection point which corresponds to the ferromagnetic temperature T_C. (b) The expanded scale of $\chi(T)$ below $x \leq 0.1$. The arrow shows the antiferromagnetic temperature T_N.

4. Discussion

We inspected the spin dynamics by applying a simple formula, which corresponds to a shift of the ac-susceptibility maxima per a frequency decade,

$$\delta T_{\mathrm{M}} = \frac{\Delta T_{\mathrm{M}}}{T_{\mathrm{M}} \Delta \log f}. \tag{1}$$

For example, the obtained δT_{M} is 0.042 for $Ce_{0.8}Er_{0.2}Al_2$. It is comparable to those reported for other metallic spin glass systems [13–17]. To investigate the nature of the spin-glass state more deeply, the well-known Vögel-Fulcher law [18] was applied to the data as follows:

$$f = f_0 \exp \frac{-E_a}{k_B (T_{\mathrm{M}} - T_0)}, \tag{2}$$

where f is the applied frequency, f_0 is the characteristic frequency; E_a is the activation energy, which determines the energetic barrier for spins to align with the external magnetic field; T_0 is the

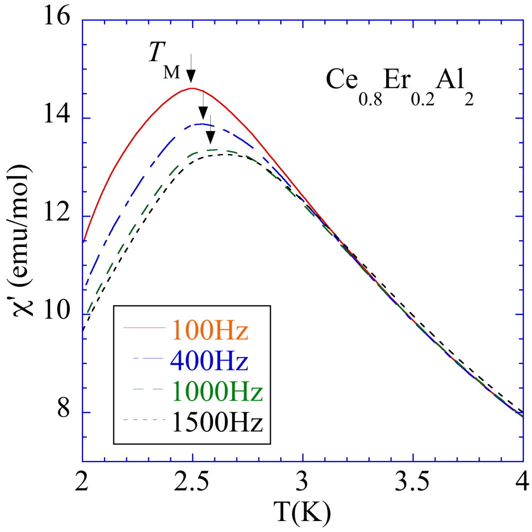

Fig. 3. Temperature dependence of ac susceptibility χ' of $Ce_{0.8}Er_{0.2}Al_2$ for several frequencies.

Vögel-Fulcher temperature, which corresponds to the interspin or intercluster interaction; and k_B is the Boltzman constant. We tested a few different f_0 values near the characteristic value 10^{13} Hz, which is typical for a spin-glass system [19]. Although the activation energies change by varying f_0, they still lie in reasonable ranges when considering the freezing temperatures. Fig. 4 shows the fit of freezing temperatures by Equation (2) in several $Ce_{1-x}Er_xAl_2$ series, where the f_0 parameter is fixed at 10^{13} Hz. The slope gives the value of the activation energy E_a. The interception with the y axis corresponds to T_0.

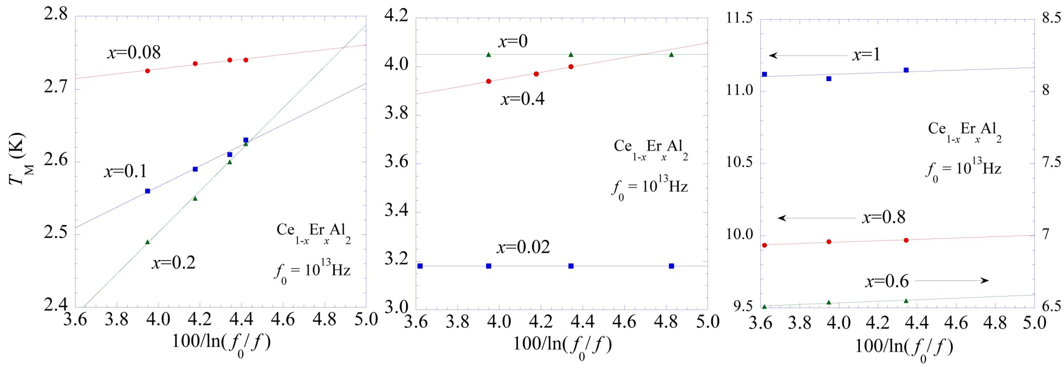

Fig. 4. Plot of T_{M} vs $100/\ln(f_0/f)$ in the $Ce_{1-x}Er_xAl_2$ series. The solid line is the least-squares fit of Equation (2). The f_0 parameter was fixed at the value of 10^{13} Hz. The obtained parameters are summarized in Fig. 5.

In Fig. 5, the obtained parameters E_a and T_0 are plotted as a function of the Er concentration x. T_0 is continuously changed as a function of Er concentration x, and shows a minimum at x = 0.2. On the other hand, it is found that the value of E_a shows a peak at x = 0.2. In general, the activation energies, E_a are of one order higher than the values of T_0 for compounds which shows the spin-glass-like behavior. For example the values of E_a and T_0 are obtained to be 39 K and 3.6 K for $PdMn_{8\%}$, and 81 K and 29.1 K for $AuFe_{10\%}$, respectively [13]. In the case of $Ce_{1-x}Er_xAl_2$, it is reasonable to assume that a spin glass behavior was found between x= 0.08 and 0.4.

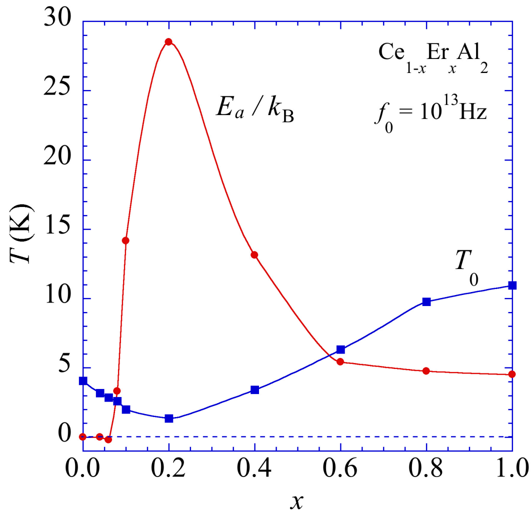

Fig. 5. The activation energy E_a and the Vögel-Fulcher temperature T_0 obtained from fitting of freezing temperatures using the Vögel-Fulcher law.

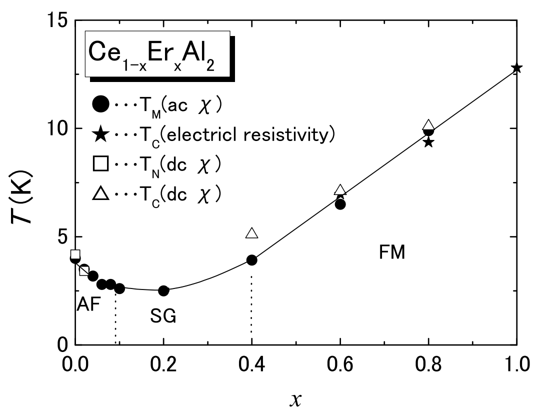

Fig. 6. Schematic phase diagram of $Ce_{1-x}Er_xAl_2$ systems.

Fig. 6 shows several characteristic temperatures considering the present data of $Ce_{1-x}Er_xAl_2$ as a function of the Er concentration x. In general, T_M, which is obtained by ac susceptibility, corresponds to Kondo temperature T_K. However, T_M can be influenced not only by the Kondo effect but also by antiferromagnetic interactions, since T_K is close to T_N which is observed in the dc-magnetic susceptibility of $CeAl_2$(x = 0). As Er concentration increases from x = 0 to 0.2, T_M decreases and the coefficient dT_M/dx approaches dT_N/dxobtained from the dc magnetic susceptibility. Between x = 0.08 and 0.4, where spin-glass like behavior is observed, the $T_M - x$ curve shows a minimum at $x \sim 0.2$. In this region, T_M corresponds to the freezing temperature. For $x > 0.2$, T_M increases with increase in x. Above x = 0.6, T_M is close to the Curie temperature T_C, which is obtained from the results of the electrical resistivity. It indicates that the ferromagnetic state is stable in this region.

5. Summary

In this work we have performed electrical resistivity, and magnetic susceptibility measurements on single crystal of $Ce_{1-x}Er_xAl_2$. A magnetic behavior was determined with a change from an antiferromagnetic ($CeAl_2$) to ferromagnetic ($ErAl_2$) ground state. The magnetic ordering temperature is continuously changed as a function of Er concentration x. A spin glass behavior was found between x= 0.08 and 0.4.

This work was supported in part by grants from The Asahi Glass Foundation, JFE 21st century Foundation, the Japan Securities Scholarship Foundation, The Kyoto Technoscience Center Foundation, JGC-S Scholarship Foundation.

References

[1] Y. Uwatoko, I. Umehara, M. Ohashi, T. Nakano and G. Oomi: *Handbook on the Physics and Chemistry of Rare Earths, Chap. 252*, ed. by K. A. Gschneidner Jr. and L. Eyring (North-Holland Amsterdam, 2012) p. 1.
[2] M. Ohashi, G. Oomi, S. Koiwai, M. Hedo, and Y. Uwatoko: Phys. Rev. B **68** (2003) 144428.
[3] M. Ohashi, G. Oomi, and I. Satoh: J. Phys. Soc. Jpn. **76** (2007) 114712.
[4] A. Iandelli and A. Palenzona: *Handbook on the Physics and Chemistry of Rare Earths, Chap. 13*, ed. by K. A. Gschneidner Jr. and L. Eyring (North-Holland Amsterdam, 1979) p. 1.
[5] H. R. Kirchmayr, C. A. Poldy, W. Steiner and G. Wiesinger: *Handbook on the Physics and Chemistry of Rare Earths, chap. 14*, ed. by K. A. Gschneidner Jr. and L. Eyring (North-Holland Amsterdam, 1979) p. 55.
[6] T. Oishi, M. Ohashi, H. Suzuki, and I. Satoh: Journal of Physics: Conference Series **200** (2010) 082022.
[7] J. C. P. Campoy, E. J. R. Plaza, A. A. Coelho, and S. Gama: Phys. Rev. B **74** (2006) 134410.
[8] E. M. Levin, V. K. Pecharsky and K. A. Geshneidner Jr.: J. Appl. Phys. **90** (2001) 6255.
[9] B. Barbara and M. F. Rossignol, J. X. Boucherle and C. Vettier: Phys. Rev. Lett. **45** (1980) 938.
[10] H. Miyagawa, G. Oomi, M. Ohashi, I. Satoh, T. Komatsubara, M. Hedo and Y. Uwatoko: Phys. Rev. B **78** (2008) 064403.
[11] S. Tomisawa, S. Wada, M. Ohashi and G.Oomi, J. Phys. : Condens Matter, **18** (2006) 10413.
[12] B. Barbara, M. F. Rossignol, J. X. Boucherle, J. Schweizer and J.L.Buevoz: J. Appl. Phys., **50** (1979) 2300.
[13] J. A. Mydosh: *Spin Glass: An Experimental Introduction* (Taylor & Francis, London 1993).
[14] D. X. Li, A. Dönni, Y. Kimura, Y. Shiokawa, Y. Homma, Y. Haga, E. Yamamoto, T. Honma and Y. Onuki: J. Phys.: Conens. Matter **11** (1999) 8263.
[15] S. Süllow, G. J. Nieuenhuys, A. A. Menovsky, J. A. Mydosh, S. A. M. Mentink, T. E. Mason and W. J. L. Buyers: Phys. Rev. Lett. **78** (1997) 354.
[16] J. Fikacek, P. Javorsky, J. Vejpravova, J. Prchal, J. Kastil, G. Nenert and E. Santava: Phys. Rev. B **85** (2012) 214410.
[17] D. X. Li, S. Nimori, Y. Shiokawa, A. Tobo, H. Onodera, Y. Haga, E. Yamamoto and Y. Onuki, Appl: Phys. Lett. **79** (2001) 4183.
[18] G. S. Fulsher: J. Am. Ceram. Soc **8** (1925) 339.
[19] J.L.Tholence, Solid State Commun.: **35** (1980) 113.